Dynamic Analysis of Piston Secondary Motion for Small Reciprocating Compressors

A. T. Prata
e-mail: prata@nrva.ufsc.br

J. R. S. Fernandes

Department of Mechanical Engineering,
Federal University of Santa Catarina,
88040-900 Florianópolis,
SC-Brazil

F. Fagotti
Brazilian Compressor Industry—EMBRACO,
89219-901 Joinville,
SC-Brazil

Piston dynamics plays a fundamental role in two critical processes related to fluid flow in reciprocating compressors. The first is the gas leakage through the radial clearance, which may cause considerable loss in the pumping efficiency of the compressor. The second process is the viscous friction associated with the lubricant film in the radial clearance. In the present contribution a numerical simulation is performed for a ringless piston inside the cylinder of a reciprocating compressor, including both the axial and the radial piston motion. The compressor considered here is a small hermetic compressor employed in domestic refrigerators, with the radial clearance between piston and cylinder filled with lubricant oil. In operation, the piston moves up and down along the axis of the cylinder, but the radial oscillatory motion in the cylinder bore, despite being usually small, plays a very important role on the compressor performance and reliability. The compromise between oil leakage through the piston-cylinder clearance and the friction losses requires a detailed analysis of the oscillatory motion for a good design. All corresponding forces and moments are included in the problem formulation of the piston dynamics in order to determine the piston trajectory, velocity and acceleration at each time step. The hydrodynamic force is obtained from the integration of the pressure distribution on the piston skirt, which, in turn, is determined from a finite volume solution of the time dependent equation that governs the oil flow. A Newton-Raphson procedure was employed in solving the equations of the piston dynamics. The results explored the effects of some design parameters and operating conditions on the stability of the piston, the oil leakage, and friction losses. Emphasis was placed on investigating the influence of the pin location, radial clearance and oil viscosity on the piston dynamics.
[S0742-4787(11)00301-8]

Keywords: Piston Dynamics, Ringless Piston, Piston Lubrication

Introduction

The forces acting on a piston as it goes up and down in a reciprocating engine are the force due to the compressed gas acting on the top of the piston, the connecting rod force, the normal force due to the hydrodynamic pressure developed in the oil film between the piston and cylinder bore, the force resulting from the piston inertia and the friction force. Those forces and the corresponding moments due to the hydrodynamic and the friction forces are represented in Fig. 1. As a result of those unbalanced forces, in addition to the piston movement up and down small translations and rotations can occur. It has long been recognized that these oscillatory motions are very important to engine performance and reliability. Therefore, all the major concern in designing those systems, such as gas leakage, frictional power loss, noise and anti-wear life, are significantly related to the mutual dependence between the piston dynamics and the lubrication. In small reciprocating compressors employed in domestic refrigerators, extremely low friction loss is required and ringless piston are commonly used to reduce the friction between the piston skirt and cylinder wall. In those ringless compressors the sealing of the pressure differential across the piston skirt is obtained by the small oil-filled radial clearance between piston and cylinder. A compromise then has to be achieved between a radial clearance that is small enough to prevent oil leakage and large enough to avoid significant friction loss. To fully benefit from lower friction and minimum leakage in a ringless piston, any contact between piston and cylinder wall must be prevented. Because of the freedom of lateral motion in ringless piston compressors, a small and stable reciprocating motion of the piston should be ensured by a thin fluid film between piston and cylinder maintained at all times. Lubrication thus plays an important role when performing a complete dynamic analysis of reciprocating pistons.

Lubrication characteristics between piston and cylinder in reciprocating motion has been a well explored topic. For a literature review before the eighties, on both theoretical and experimental attempts to explore piston lubrication, reference is made to Li et al. [1]. Those authors themselves have shown through an analytical model that piston skirt friction can be significantly increased if the wrist-pin is located in an unfavorable position. A brief survey, focusing on those contributions relevant to the present investigation will now be presented.

A numerical study on piston slap in diesel engines was performed by Suzuki et al. [2] who explored the effects of arbitrary skirt surfaces and pin eccentricity in the piston dynamics. Zhu et al. [3,4] numerically investigated piston motion, lubrication, and friction in mixed lubrication taking into account effects of surface waviness, roughness, surface profile, bulk elastic deformation, and thermal distortion of both piston skirt and cylinder bore. The proposed model was applied to a four stroke automotive engine showing that good hydrodynamic lubrication can minimize the possibility and severeness of piston impact against the cylinder bore and reduce the frictional loss.

In a sequence of three papers, Gommed and Etsion [5,6] and Etsion and Gommed [7] presented a mathematical model for analyzing the dynamics of gas lubricated ringless pistons. A relatively large size helium cryocooler was investigated and it was shown that although a cylindrical piston shape is commonly used for ringless piston applications, this is not the best choice for an op-

Contributed by the Tribology Division for publication in the ASME JOURNAL OF TRIBOLOGY. Manuscript received by the Tribology Division December 21, 1999; revised manuscript received April 4, 2000. Associate Technical Editor: J. Frêne.

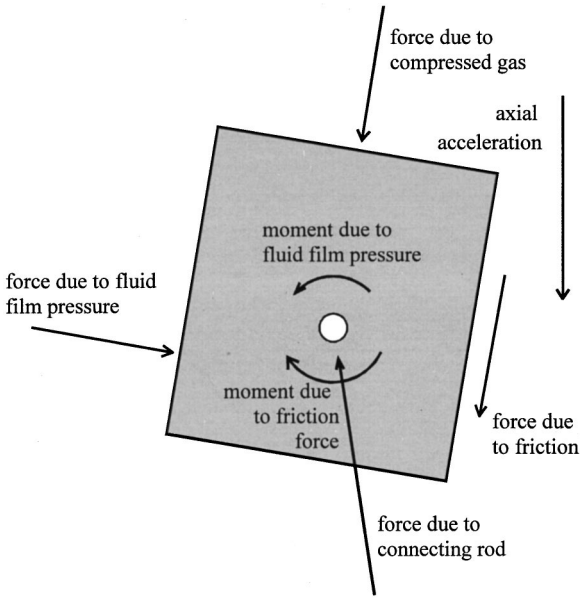

Fig. 1 Force and moments acting on a piston

timum design as far as piston stability and sealing performance are concerned. Other piston shapes were explored and an improved design was obtained with noncylindrical profiles.

Theoretical and experimental results were obtained by Yamaguchi [8] for two piston-cylinder assemblies. One operating in the standard mode, with hydrodynamic lubrication, and other operating in hydrostatic lubrication with oil being injected in the radial clearance between piston and cylinder. It was shown for low crankshaft velocities, that the hydrostatic piston can operate with reduced friction and same oil leakage as the hydrodynamic piston as long as the radial clearance is made small.

Lee [9] proposed a piston with tilted top for an internal combustion engine that is able to employ the combustion gas force in favor of the piston stability. Elastohydrodynamic lubrication was investigated by Dursunkaya et al. [10] for a diesel engine. It was shown that surface deformation can play a significant role in the piston secondary motion.

Mixed lubrication between piston and cylinder in a hydraulic piston pump-motor was investigated by Fang and Shirakashi [11]. The metal contact between the parts was expressed in terms of a contact ratio defined as the percentage of the period with contact to the whole period of stroke. It was shown that curves of contact ratio versus the ratio of dynamic pressure due to wedge effect to the supply pressure in the cylinder are effective in expressing the characteristics of mixed lubrication for this type of system.

Liu et al. [12] performed a mixed lubrication model for a piston-cylinder assembly and showed that a parabolic piston skirt profile considerably reduces the friction power loss and substantially improves lubrication in both the up and down strokes.

The present work deals with oil lubrication in ringless reciprocating compressors. The main objective here is to perform a dynamic analysis for the thin oil film between piston and cylinder in presence of oscillatory secondary motion occurring in small refrigerating compressors. The complete set of equations describing both piston and connecting rod motion are employed in the formulation, allowing the prediction of the spatial and time varying radial clearance, required for the lubrication equation.

For the typical hermetic compressor being considered here, the bottom of the compressor shell is filled with oil and the shaft lays vertically with its lower part immersed in the lubricant [13]. During operation an helicoidal channel drives the oil along the shaft from the swamp to the top where the connecting rod is assembled. Oil is then abundantly sprinkled at the cylinder wall, the piston base, and the wrist-pin. Oil is also carried into the cylinder through the compressor suction, because gas suction occurs from the shell environment which is laden with small oil droplets. All that assures a flooded lubrication within the radial clearance between piston and cylinder. Visualizations made with compressors having some of their parts fabricated with transparent thermoplastic provided a further support for the flooded lubrication hypothesis assumed throughout the present analysis.

Problem Formulation

A typical piston-cylinder system encountered in small reciprocating compressors is depicted in Fig. 2. The piston, with radius R and length L is driven in a reciprocating motion by the action of the crankshaft and connecting rod. The cycle starts at the bottom dead center where $\tau = 0$ deg and ends at the same point with $\tau = 360$ deg after one revolution of the crankshaft which is rotating with an angular speed of ω. The crankshaft is located at a distance ''d'' from the cylinder axis.

The gas pressure p_{cyl} and p_{suc}, above and below the piston, respectively, are known. For the type of application being considered here, p_{suc} is the compressor suction pressure and is assumed to be constant. On the top of the piston, the pressure p_{cyl} is a known function of time. A typical variation of pressure with time

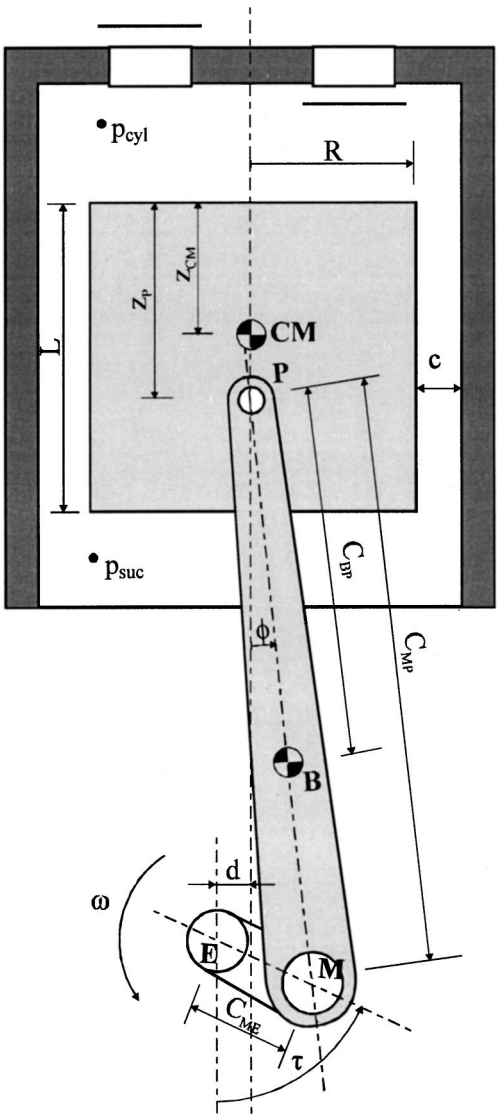

Fig. 2 Piston-cylinder system

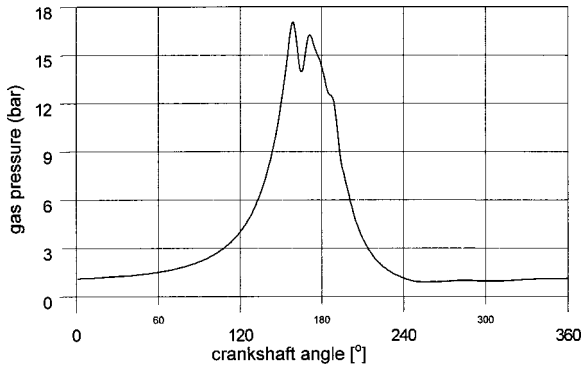

Fig. 3 Typical instantaneous gas pressure acting on piston top

is presented in Fig. 3. Those curves can be experimentally determined, as is the case in Fig. 3, calculated from thermodynamic models, which is the standard procedure in compressors simulation codes (Fagotti et al. [13], Todescat et al. [14]), or computed from energy and momentum equations (Catto and Prata [15]).

Piston orientation within the cylinder bore are shown in Fig. 4. As discussed previously, unbalanced forces acting on the piston can cause rotary and translatory motions within the confinement of the cylinder clearance. Only rotation is shown in Fig. 4. The piston location can be described by the top and bottom skirt eccentricities, e_t, and e_b, respectively, with respect to the cylinder axis. The radial velocities of the top and bottom parts of the piston skirt are, respectively, $\dot{e}_t$ and $\dot{e}_b$; the corresponding accelerations are $\ddot{e}_t$ and $\ddot{e}_b$. It should be noted that e_t and e_b are functions of time and should be predicted by solving the piston equations of motion. The use of e_t and e_b in describing the piston location is equivalent of using the eccentricity measured from the cylinder

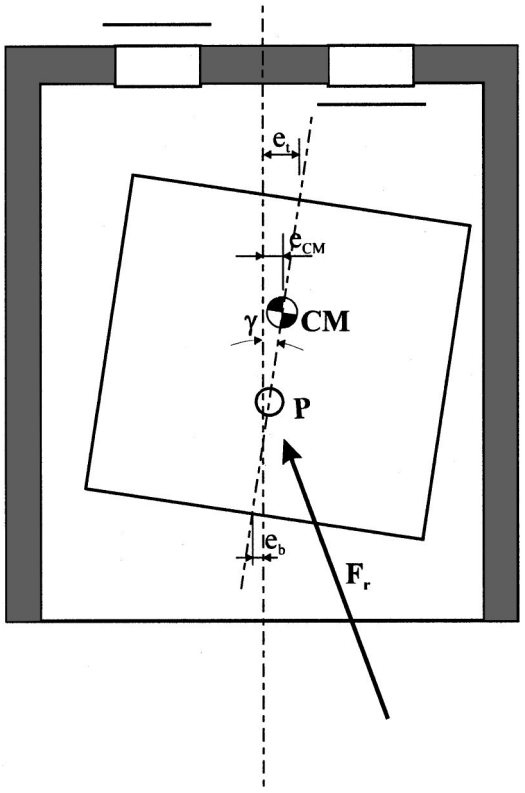

Fig. 4 Piston orientation within the cylinder bore

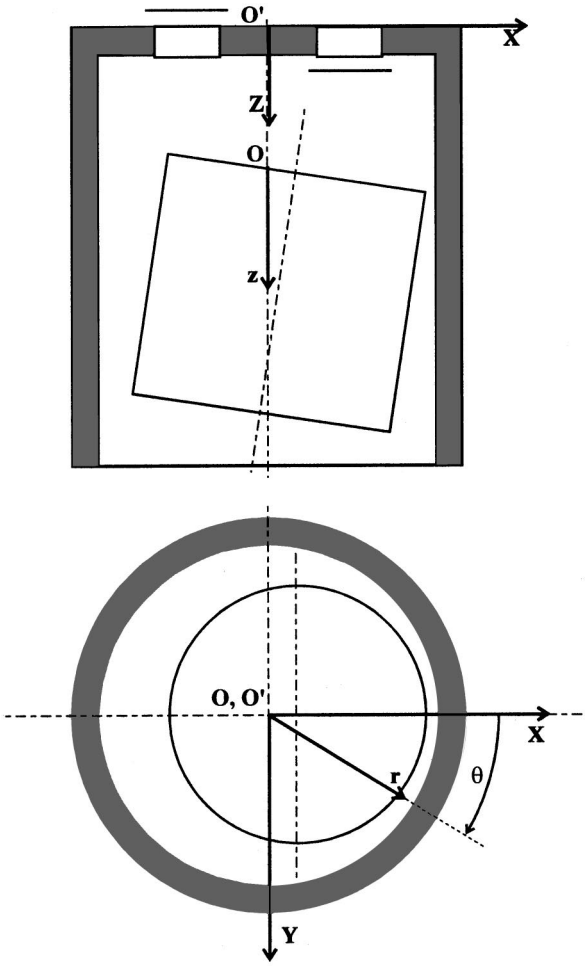

Fig. 5 Coordinate systems employed in the solution of the problem

axis to the center of mass of the piston, e_{CM}, and the tilt angle γ with respect to the cylinder axis (Gommed and Etsion [5]). The piston axial velocity and acceleration are V_p and A_p, respectively. All the motions (rotation, radial and axial translation) take place in a plane parallel to the cylinder axis and perpendicular to the wrist-pin axis.

Two coordinate systems shown in Fig. 5 are employed in solving the problem. System *XYZ* has its origin, O', fixed at the cylinder top; the *Z* direction coincides with the cylinder axis, and *X* lies on the plane of the piston motion. The system *XYZ* is used to formulate the equations governing the piston dynamics. Another coordinate system, $r\theta z$, has its origin, *O*, at the top of the piston and moves with the piston velocity V_p. The moving polar system, $r\theta$, is parallel to the *XY* plane of the fixed system, *XYZ*, and is employed to calculate the hydrodynamic induced pressure throughout the radial clearance.

In writing the governing equations of the problem, some basic assumptions are adopted. First it is assumed that the radial clearance *c*, shown with exaggerated dimension in Figs. 2, 4, and 5, is much smaller than the piston radius. Thus, radial variation of pressure in the fluid film is negligible. Furthermore, all solid parts are rigid, and no deformation occurs. The oil flow is laminar and because the radial clearance is much smaller than the piston length, *L*, entrance effects are ignored. Oil is considered to be a Newtonian isoviscous fluid with all properties constant, and a flooded lubrication condition is assumed.

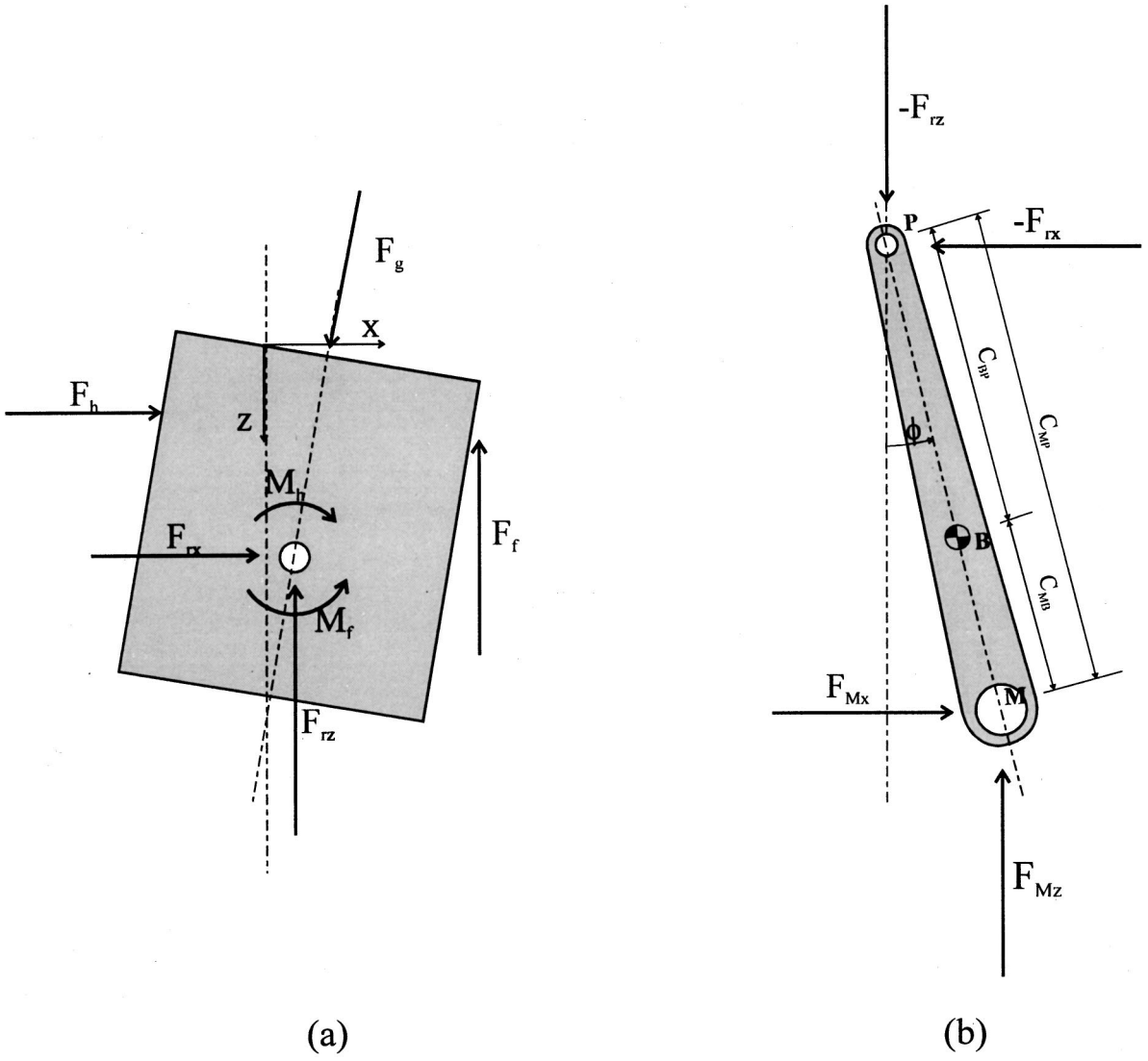

Fig. 6 Free-body diagram for (*a*) piston, and (*b*) connecting rod

With the aid of Figs. 1 and 4, and considering that all motions occur in plane *XY* as indicated in Fig. 5, the equations describing the piston dynamics can be written as,

$$F_h + F_{rx} = m\ddot{e}_{CM} \tag{1}$$

$$F_g + F_f + F_{rz} = mA_p \tag{2}$$

$$M_h + M_f = I_P \ddot{\gamma}, \tag{3}$$

where F_h is the hydrodynamic force due to the pressure in the oil film, F_g is the gas force acting on the top of the piston, F_f is the viscous friction force due to the oil movement within the radial clearance, F_{rz} and F_{rx} are, respectively, the axial and radial components of the connecting rod force, m is the piston mass, I_p is the piston moment of inertia about the wrist-pin location, M_h and M_f are, respectively, the moments about the wrist-pin due to F_h and F_f, and $\ddot{\gamma}$ is the piston rotary acceleration about the wrist-pin. Because γ in Fig. 4 is very small, F_g and F_f are considered to be aligned with the Z axis, and F_h aligned with the X axis.

Due to the option of working with radial accelerations at the top and bottom of the piston, $\ddot{e}_t$ and $\ddot{e}_b$, respectively, instead of $\ddot{e}_{CM}$ and $\ddot{\gamma}$, the following equations are employed:

$$\ddot{\gamma} = (\ddot{e}_t - \ddot{e}_b)/L = c\omega^2(\ddot{\varepsilon}_t - \ddot{\varepsilon}_b)/L \tag{4}$$

$$\ddot{e}_{CM} = \ddot{e}_t - Z_{CM}\ddot{\gamma} = c\omega^2[\ddot{\varepsilon}_t - Z_{CM}(\ddot{\varepsilon}_t - \ddot{\varepsilon}_b)/L]. \tag{5}$$

In writing Eqs. (4) and (5), the time derivative was exchanged by the derivative with respect to the angle τ, where $d\tau = \omega dt$. Also, use was made of $\varepsilon_t = e_t/c$ and $\varepsilon_b = e_b/c$, the dimensionless eccentricities of the top and bottom of the piston, respectively.

To determine the connecting rod forces acting on the piston, F_{rx} and F_{rz}, the equations governing the connecting rod dynamics are required. To this extent, making use of the free-body diagram for the connecting rod shown in Fig. 6, the following equations can be written:

$$F_{Mx} - F_{rx} = m_b A_{Bx} \tag{6}$$

$$F_{Mz} - F_{rz} = m_b A_{Bz} \tag{7}$$

$$(F_{rz}C_{BP} + F_{Mz}C_{MB})\sin\phi - (F_{Mx}C_{MB} + F_{rx}C_{BP})\cos\phi = I_B\ddot{\phi} \tag{8}$$

In Eqs. (6)–(8), F_{Mx} and F_{Mz} are the radial and axial components of the crankshaft force acting on the connecting rod, m_b is the connecting rod mass, A_{Bx} and A_{Bz} are, respectively, the radial and axial components of the connecting rod acceleration, C_{BP} and C_{MB} are, respectively, the distance between the connecting rod

center of mass to P and to M, as indicated in Fig. 6; ϕ and $\ddot{\phi}$ are, respectively, the connecting rod tilting angle with respect to the cylinder axis and its angular acceleration; I_B is the connecting rod moment of inertia with respect to its center of mass, B.

The hydrodynamic force, F_h, acting on the piston skirt due to the pressure developed in the oil film, is to be obtained from the Reynolds equation. For the present situation the Reynolds equation can be written as

$$\frac{\partial}{\partial\theta}\left(h^3\frac{\partial p}{\partial\theta}\right)+\frac{\partial}{\partial\xi}\left(h^3\frac{\partial p}{\partial\xi}\right)=-12\mu R^2\left(\frac{V_p}{2R}\frac{\partial h}{\partial\xi}-\frac{\partial h}{\partial t}\right), \quad (9)$$

where $\xi=z/R$, μ is the oil viscosity and h is the local oil film thickness. For an eccentric and tilted piston, h can be obtained from

$$h=c\left\{1-\left[\varepsilon_t-(\varepsilon_t-\varepsilon_b)\xi\frac{R}{L}\right]\cos\theta\right\}. \quad (10)$$

Associated to Eq. (9), the following boundary conditions are employed:

$$\xi=0,\ p=p_{\text{cyl}} \quad \text{and} \quad \xi=L/R,\ p=p_{\text{suc}} \quad (11)$$

in which p_{cyl} and p_{suc} are the pressure above and below the piston, respectively, as previously discussed. Along the θ direction, a full circumferential oil film is considered and a periodic boundary condition is imposed, $p(\theta)=p(\theta+2\pi\theta)$. Symmetry along θ was not employed here allowing for more generality of the computer code being developed.

Once the pressure in the oil film is known, both F_h and M_h can be determined from, respectively,

$$F_h=-\int_0^L\int_0^{2\pi}p(\theta,z)R\cos\theta\,d\theta dz \quad (12)$$

and

$$M_h=-\int_0^L\int_0^{2\pi}[p(\theta,z)R\cos\theta](z_p-z)\,d\theta dz, \quad (13)$$

where z_p is the wrist-pin location from the top of the piston. It should be noted that the $\cos\theta$ appears in both Eqs. (12) and (13) because piston motion is allowed only on the plane that is parallel to the cylinder axis and perpendicular to the wrist-pin axis.

From the piston motion and oil flow, the viscous frictional force and moment may be computed according to

$$F_f=-\int_0^L\int_0^{2\pi}\left(\frac{h}{2}\frac{\partial p}{\partial z}+\mu\frac{V_p}{h}\right)R\,d\theta dz \quad (14)$$

and

$$M_f=-\int_0^L\int_0^{2\pi}\left(\frac{h}{2}\frac{\partial p}{\partial z}+\mu\frac{V_p}{h}\right)R\cos\theta\cdot R\,d\theta dz, \quad (15)$$

respectively.

The force due to the compressed gas, F_g is simply,

$$F_g=\pi R^2(p_{\text{cyl}}-p_{\text{suc}}) \quad (16)$$

At this moment, the problem formulation has been completed. The kinematics of crankshaft-connecting rod system yields expressions for determining the piston velocity and acceleration, V_P and A_P, respectively, as well as the components A_{BX} and A_{BZ} of the connecting rod acceleration, and the connecting rod tilting angle, ϕ, together with its acceleration, $\ddot{\phi}$. All those quantities are to be expressed in terms of the crankshaft angle, τ.

Mathematical Model

The equations for the piston and connecting rod dynamics, Eqs. (1)–(3) and (6)–(8), respectively, can be combined into only two differential equations. To that extent, F_{rz} from Eq. (2) is first substituted into Eq. (7), resulting in an equation for F_{Mz} in terms of F_g and F_f. Next, F_{Mx} from Eq. (6) is substituted into Eq. (8) yielding, after substitution for the previous equation for F_{rz} and F_{Mz}, the following equation:

$$F_{rx}=[(mA_P-F_g-F_f)C_{BP}+(m_bA_{Bz}+mA_P-F_g-F_f)C_{MB}) \pm C_{MB}m_bA_{Bx}-I_B\ddot{\phi}/\cos\phi]/(C_{MB}+C_{BP}). \quad (17)$$

Now, substituting Eqs. (4) and (5) into Eqs. (1) and (3), respectively, results in

$$F_h+F_{rx}=mc\omega^2[\ddot{\varepsilon}_t-z_{CM}(\ddot{\varepsilon}_t-\ddot{\varepsilon}_b)/L] \quad (18)$$

$$M_h+M_f=I_pc\omega^2(\ddot{\varepsilon}_t-\ddot{\varepsilon}_b)/L. \quad (19)$$

The piston trajectory in terms of e_t and e_b as a function of the crankshaft angle τ can now be calculated from Eqs. (18) and (19). Required in those equations are F_h, F_{rx}, M_h, and M_f, which can be obtained, respectively, from Eqs. (12), (17), (13), and (15).

Numerical Methodology

The numerical solution of Eqs. (18) and (19) starts with prescribed values for e_t, e_b, $\dot{e}_t$, and $\dot{e}_b$. Because the piston trajectory inside the cylinder is periodic, the converged solution should not depend on the initial guess. For simplicity it is assumed that, at $\tau=0$, $e_t=e_b=\dot{e}_t=\dot{e}_b=0$.

An implicit formulation is employed here and from the initial values the crankshaft angle is advanced and from the geometrical parameters and the equations for the kinematics of the crankshaft-connecting rod system, values of piston velocity and acceleration along Z and connecting rod acceleration are determined for $\tau+\Delta\tau$. From Fig. 3, p_{cyl} for $\tau+\Delta\tau$ is also obtained. An iterative process is then needed to determine the piston radial position and velocity at time $\tau+\Delta\tau$, that is $\varepsilon_t^{\tau+\Delta\tau}$, $\varepsilon_b^{\tau+\Delta\tau}$, $\dot{\varepsilon}_t^{\tau+\Delta\tau}$, $\dot{\varepsilon}_b^{\tau+\Delta\tau}$. This is performed using a Newton-Raphson procedure to search for the $\dot{\varepsilon}_t^{\tau+\Delta\tau}$ and $\dot{\varepsilon}_b^{\tau+\Delta\tau}$ values that would satisfy Eqs. (18) and (19). Values of both piston radial position and acceleration are obtained from the radial velocities $\dot{\varepsilon}_t^{\tau}$ and $\dot{\varepsilon}_b^{\tau}$ as

$$\varepsilon_t^{\tau+\Delta\tau}=\varepsilon_t^{\tau}+\dot{\varepsilon}_t^{\tau+\Delta\tau}\cdot\Delta\tau, \quad \varepsilon_b^{\tau+\Delta\tau}=\varepsilon_b^{\tau}+\dot{\varepsilon}_b^{\tau+\Delta\tau}\cdot\Delta\tau \quad (20)$$

$$\ddot{\varepsilon}_t^{\tau+\Delta\tau}=(\dot{\varepsilon}_t^{\tau+\Delta\tau}-\dot{\varepsilon}_t^{\tau})/\Delta\tau, \quad \ddot{\varepsilon}_b^{\tau+\Delta\tau}=(\dot{\varepsilon}_b^{\tau+\Delta\tau}-\dot{\varepsilon}_b^{\tau})/\Delta\tau. \quad (21)$$

The pressure field required in both Eqs. (14) and (15) to calculate F_f and M_f, respectively, is determined integrating Eq. (9) through a finite volume approach (Prata and Ferreira [16]). In some situations, nonrealistic pressure values may be obtained from Eq. (9). Because the oil film cannot sustain pressure values smaller than the gas pressure at the edges of the piston skirt, gaseous cavitation occurs (Dowson and Taylor [17]). In turn, the continuity of the oil film is lost and striae are observed in the oil flow pattern. In the present work, whenever cavitation occurred, the oil pressure was replaced by a gas pressure interpolated between p_{cyl} and p_{suc}, depending on the cavitation axial location.

For the numerical solution, a typical time step corresponding to five degrees of the crankshaft angle was employed for most calculations. Test runs indicated that for smaller time step lengths less iterations were required to achieve convergence at each time interval. When a time step corresponding to 0.5 degrees of the crankshaft angle was employed, only two iterations at each time step was sufficient. Convergence of the Newton-Raphson algorithm at each time step was achieved at most in ten iterations. A converged periodic solution for the piston trajectory required about 30 cycles. Several tests were performed to validate the numerical code. Worth mentioning is that the work delivered to the compressed gas obtained from the area of the pv diagram constructed using the gas pressure from Fig. 3 when added to the energy required to overcome friction, obtained from the viscous frictional force given by Eq. (14) and the instantaneous piston velocity, agreed within 0.02 percent with the computed work delivered to the connecting rod from the crankshaft and obtained through kinematics considerations.

Results and Discussions

The results to be presented were obtained for a typical reciprocating compressor employed in domestic refrigerators. Some input data including geometric parameters of the compressor is listed in Table 1.

The first results to be presented focus on the forces acting on the piston as it moves up and down. Figures 7(*a*) and (*b*) present the forces along the radial and axial directions, respectively, for a complete piston cycle. A minor role is played by the inertial force, $F_i(=-m\ddot{e}_{CM})$, as observed from the figures; along the radial direction the influence of inertia on the piston dynamics is virtually none. Comparing Figs. 7(*a*) and (*b*), it is seen that along the axial direction the forces are one order of magnitude higher than those along the radial direction. For both directions the forces reach their highest values close to the top dead center ($\tau=180$ deg). The connecting rod force, F_r, is balanced mainly by the hydrodynamic force along the radial direction and by the gas force along the axial direction. From Fig. 7(*b*) it is also seen that the friction force, F_f, is negligible. A further comment should be made with respect to the oscillation of both F_g and F_{rz} close to the top dead center. This behavior is related to the oscillation of the compressor discharge pressure as shown in Fig. 3, and is due to valve fluttering.

Table 1 Geometric, dynamic, and operational baseline parameters used in the simulation

R (mm)	10.5
c (μm)	5.0
L* (L/R)	2
z_P* (z_P/R)	1.150
z_{CM}* (z_{CM}/R)	1.053
C_{BP}* (C_{BP}/R)	2.431
C_{MP}* (C_{MP}/R)	3.473
C_{ME}* (C_{ME}/R)	0.6857
d* (d/R)	0.1905
ω (rd/s)	368.6
p_{suc} (bar)	1.156
μ (Pa.s)	0.0024
m (g)	34.1
m_b (g)	23.6
I_P^* [$I_P/(mR^2)$]	0.6038
I_B^* [$I_B/(m_bC_{MP}^2)$]	0.1896

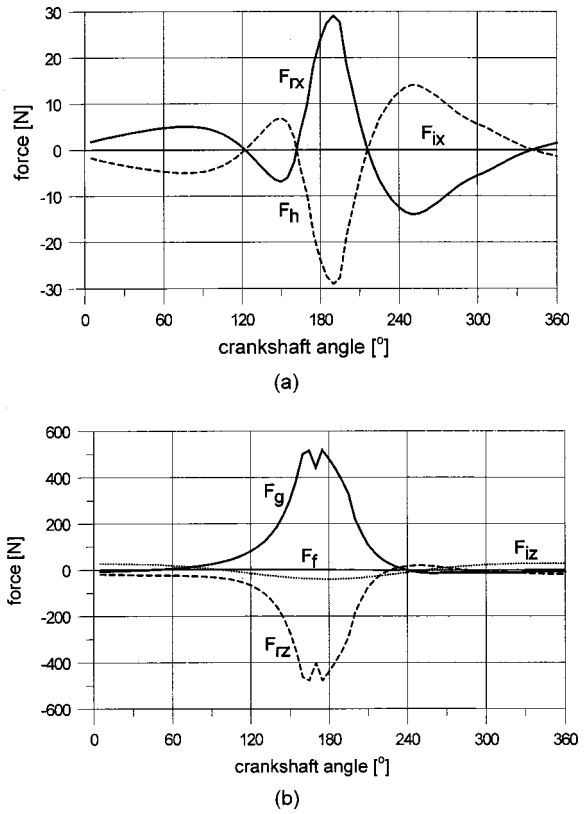

Fig. 7 Forces acting on the piston as a function of crankshaft angle: (*a*) radial; (*b*) axial

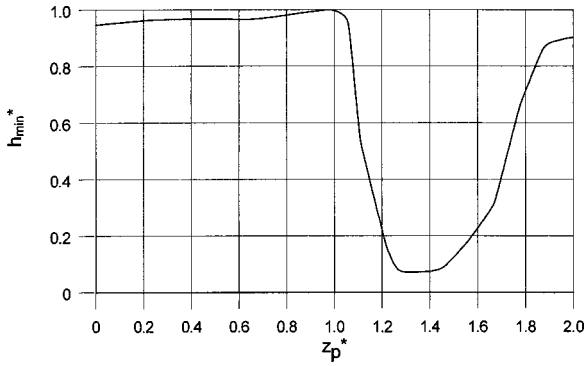

Fig. 8 Minimum local oil film thickness during a cycle as a function of wrist-pin location

Attention will now be turned to the influence of some design parameters on the piston trajectory within the cylinder. Variation of the minimum dimensionless distance between piston and cylinder, $h^*_{\min}=h_{\min}/c$, with respect to the dimensionless wrist-pin location, $z_p^*=z_p/R$, is presented in Fig. 8. At $z_p^*=1$, the wrist-pin is located at the midpoint between top and bottom of the piston. From the figure it is seen that at this location $h^*_{\min}$ has its maximum value indicating the condition of highest stability. This tendency is in close relation to the behavior of the acting moments on the piston throughout a cycle: at $z_p^*=1$ the moments have their smallest values.

To decide about the optimum wrist-pin location the results of Fig. 8 have to be analyzed in conjunction with results for oil leakage and power consumption. In addition to oil consumption information, oil leakage between piston skirt and cylinder bore is very important in assessing refrigerant leakage, which occurs because of the gas solubility in the oil. Gas dissolved in the oil plays an important role in reducing the compressor volumetric efficiency. The description of the different models for assessing gas losses from oil leakage is beyond the scope of the present work and can be found elsewhere [18,19].

The instantaneous volumetric oil leakage throughout the clearance between piston and cylinder is given by

$$V_\tau=\int_0^{2\pi}\left(\frac{-h^3}{12\mu R}\frac{\partial p}{\partial \xi}+V_P\frac{h}{2}\right)\Bigg|_{z=L} R\,d\theta. \tag{22}$$

From that, cycle average leakage can be obtained from

$$V=\frac{1}{2\pi}\int_0^{2\pi} V_\tau\,d\tau. \tag{23}$$

Similarly, a cycle averaged power consumption can be calculated from

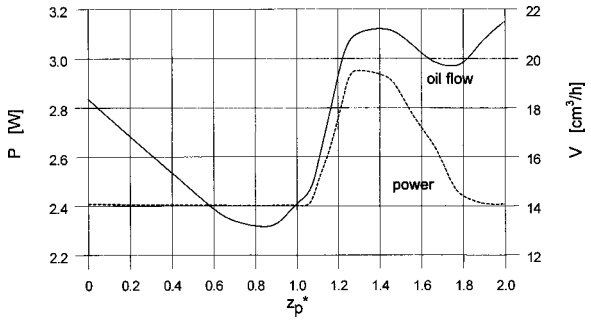

Fig. 9 Averaged power consumption and averaged oil leakage as a function of wrist-pin location

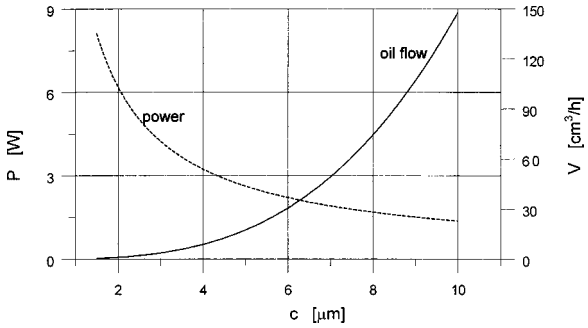

Fig. 11 Averaged power consumption and averaged oil leakage as a function of skirt-to-bore radial clearance

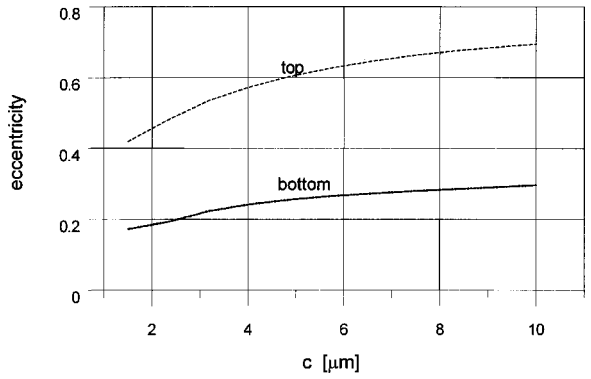

Fig. 10 Maximum eccentricity of top and bottom during a cycle as a function of skirt-to-bore radial clearance

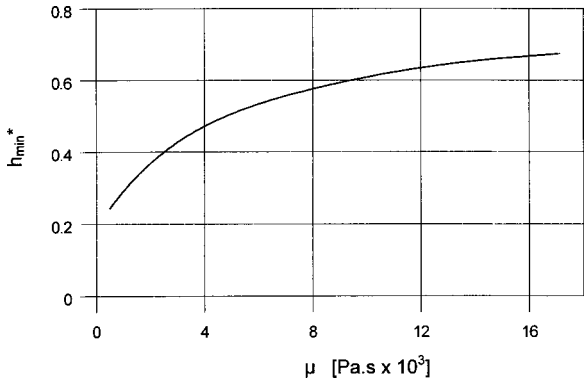

Fig. 12 Minimum local oil film thickness during a cycle as a function of lubricant viscosity

$$P=\frac{1}{2\pi}\int_0^{2\pi} P_\tau\, d\tau, \quad P_\tau = F_f V_P, \tag{24}$$

where P_τ is the instantaneous power consumption obtained from the friction force F_f, Eq. (14), and piston velocity V_P.

Integration of Eqs. (14) and (22) were performed numerically visiting all control volumes of the computational mesh. Because of cavitation, control volumes located in regions void of lubricant were disregarded during the integration.

Results for the power consumption, P, and the volumetric oil leakage, V, are shown in Fig. 9. From Figs. 8 and 9 it is seen that optimum wrist-pin location lies between $z_p^*=0.8$ and 1.0. At this range of z_p^*, the piston operates in a stable trajectory, with low leakage and low frictional power loss.

The increase in oil leakage for values of z_p^* greater than one, as seen in Fig. 9, coincides with the more unstable pattern for the piston motion observed in Fig. 8 for the same z_p^* values. This is so because the increase in oil leakage due to increasing values of the radial clearance at some location more than compensates for the decrease in oil leakage due to the resulting decrease in the radial clearance at the opposite locations as the piston oscillates.

The oil leakage is strongly affected by the pressure field in the oil film within the clearance. As the wrist-pin location is altered, higher pressure gradients may occur closer or farther the piston edges, regardless of the piston oscillation. That could possibly explain the large oil flow for z_p^* near the piston top and bottom, despite the minimum clearance value close to unity. It should be noted, however, that the relationship among pressure gradient, pin position, and piston location is rather complex preventing a detailed interpretation of the curves presented in Figs. 8 and 9.

The influence of the radial clearance between piston skirt and cylinder bore on the maximum value of the dimensionless eccentricity of the top and bottom during a cycle is presented in Fig. 10.

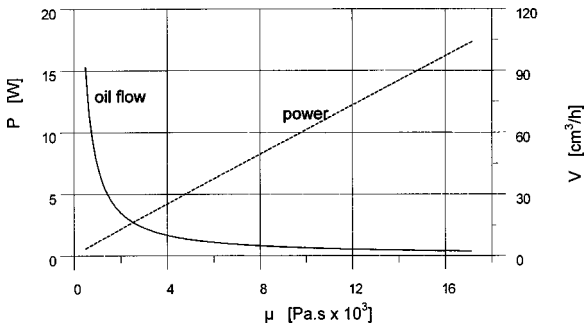

Fig. 13 Averaged power consumption and averaged oil leakage as a function of lubricant viscosity

As seen from the figure, the piston becomes more unstable as the radial clearance is increased, which was also observed by Li et al. [1], Zhu et al. [3] and Gommed and Etsion [6]. Smaller values of clearance c result in increasing damping of the oil film which, in turn, tend to stabilize the piston.

From the stability point of view, the smaller the radial clearance the better the design. However, as shown in Fig. 11, small values of c results in considerable demand for power to overcome viscous friction. From Fig. 11, it is seen that a compromise can be achieved between power consumption and oil leakage, which is around $c=6$ μm. At this value Fig. 10 yields maximum eccentricities of 0.63 and 0.27 for top and bottom of piston skirt, respectively.

The effect of lubricant viscosity on the minimum dimensionless distance between piston and cylinder, $h_{\min}^*$, is presented in Fig. 12. As would be expected, the stability of the piston trajectory increases as the viscosity increases. Despite the benefit of higher stability as oil viscosity is increased, viscous friction should also

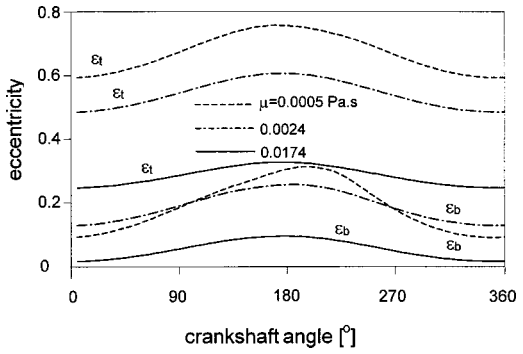

Fig. 14 Effect of oil viscosity on top and bottom eccentricity ratios as a function of crankshaft angle

be considered. As seen in Fig. 13, the averaged power consumption per cycle increases almost linearly with the oil viscosity. Also shown in Fig. 13 is the averaged oil leakage as a function of the lubricant viscosity. From the figure it is observed that viscosity plays a very important role on oil leakage for a small range of μ values. As μ is increased, the oil leakage tend to be less and less affected by viscosity.

The influence of the oil viscosity on the radial oscillatory motion of the piston is presented in Fig. 14 for an entire cycle. From the figure it is seen that higher viscosities tend to damp out the radial oscillation. For the lowest viscosity investigated the piston bottom tends to oscillate more than the piston top. This is so because for the reference case considered the wrist-pin is located below the piston center, facilitating the lubrication restoring effect on the lower part of the piston.

Conclusions

A dynamic model for piston lubrication for small reciprocating compressors was presented. Oscillatory secondary piston motion due to the unbalanced forces acting on the piston plays an important role on compressor performance and was shown to significantly affect both power consumption and oil leakage between piston skirt and cylinder bore.

The analysis incorporated equations for both piston and connecting rod dynamics as well as the lubrication equation applied to the variable shape oil film present within the confinement of the skirt-to-bore radial clearance.

Results for piston trajectory, power consumption and oil leakage were explored as a function of wrist-pin location, radial clearance between piston and cylinder, and lubricant viscosity. Among the results it was shown that undesirable piston oscillation can be significantly increased if the wrist-pin is placed below the middle of the skirt. At this location the power consumption and oil leakage presented their highest values.

There are many parameters and factors that affect piston performance which were not explored here. The model presented can be used as helpful tool in assessing the influence of length, mass, shape and location of center of mass of the piston, just to mention a few parameters. Other studies can also be performed to investigate whether a lateral wrist-pin offset can be beneficial in decreasing the moments acting on the piston which would improve piston stability. Further improvements in the present model should incorporate piston and cylinder deformation, as well as skirt and cylinder contact and friction.

Nomenclature

A_{BX} = connecting rod acceleration along X, m/s^2
A_{BZ} = connecting rod acceleration along Z, m/s^2
A_P = piston axial acceleration, m/s^2
c = radial clearance between piston and cylinder, μm
C_{BP} = distance between wrist-pin and connecting rod center of mass, m
C_{MB} = connecting rod length, m
d = distance between connecting rod axis and cylinder axis, m
e_{CM} = eccentricity of piston center of mass, m
e_t = piston top eccentricity, m
e_b = piston bottom eccentricity, m
F_f = viscous friction force, N
F_g = gas force, N
F_h = hydrodynamic force, N
F_i = inertial force, N
F_M = crankshaft force, N
F_r = connecting rod force, N
h = local oil film thickness, m
$h_{\min}$ = minimum distance between piston and cylinder during a cycle, m
I_B = connecting rod moment of inertia about its center of mass, kg·m^2
I_P = piston moment of inertia about wrist-pin, kg·m^2
L = piston length, m
m = piston mass, kg
m_b = connecting rod mass, kg
M_f = viscous moment about wrist-pin, N·m
M_h = hydrodynamic moment about wrist-pin, N·m
p = oil film pressure, Pa
P = cycle averaged power consumption by viscous friction, W
P_τ = instantaneous power consumption by viscous friction, W
r = radial coordinate, m
R = piston radius, m
V = cycle averaged volumetric oil leakage, cm^3/h
V_P = piston velocity, m/s
z = axial coordinate, m
z_P = wrist-pin location from the top of the piston, m

Greek Symbols

ε = dimensionless eccentricity
ϕ = angle between connecting rod and cylinder axis
γ = piston tilt angle
μ = viscosity of lubricant oil, Pa·s
θ = angular coordinate
τ = crankshaft angle
ω = crankshaft angular velocity ($\omega = d\tau/dt$), rad/s
ξ = dimensionless distance along z ($\xi = z/R$)

References

[1] Li, D. F., Rohde, S. M., and Ezzat, H. A., 1983, ''An Automotive Piston Lubrication Model,'' ASLE Trans., **26**, No. 2, pp. 151–160.
[2] Suzuki, T., Fujimoto, Y., Ochiai, Y., and Fujimura, I., 1987, ''A Numerical Study on Piston Slap in Diesel Engines,'' JSME Transactions, Ser. B, **53**, pp. 2610–2618.
[3] Zhu, D., Cheng, H. S., Takayuki, A., and Hamai, K., 1992, ''A Numerical Analysis for Piston Skirts in Mixed Lubrication: Part I—Basic Modeling,'' ASME J. Tribol., **114**, pp. 553–562.
[4] Zhu, D., Hu, Y., Cheng, H. S., Takayuki, A., and Hamai, K., 1993, ''A Numerical Analysis for Piston Skirts in Mixed Lubrication: Part II—Deformation Considerations,'' ASME J. Tribol., **115**, pp. 125–133.
[5] Gommed, K., and Etsion, I., 1993, ''Dynamic Analysis of Gas Lubricated Reciprocating Ringless Pistons—Basic Modeling,'' ASME J. Tribol., **115**, pp. 207–213.
[6] Gommed, K., and Etsion, I., 1994, ''Parametric Study of the Dynamic Performance of Gas Lubricated Ringless Pistons,'' ASME J. Tribol., **116**, pp. 63–69.
[7] Etsion, I., and Gommed, K., 1995, ''Improved Design with Noncylindrical Profiles of Gas-Lubricated Ringless Piston,'' ASME J. Tribol., **117**, pp. 143–147.
[8] Yamaguchi, A., 1994, ''Motion of the Piston in Piston Pumps and Motors,'' JSME Int. J., Ser. B, **37**, No. 1, pp. 83–88.
[9] Lee, H., 1994, ''High Performance Internal Combustion Engine With Gas-Cushioned Piston,'' JSME Int. J., Ser. B, **37**, No. 2, pp. 434–442.
[10] Dursunkaya, Z., Keribar, R., and Ganapathy, V., 1994, ''A Model of Piston Secondary Motion and Elastohydrodynamic Skirt Lubrication,'' ASME J. Tribol., **116**, pp. 777–785.

[11] Fang, Y., and Shirakashi, M., 1995, ''Mixed Lubrication Characteristics Between the Piston and Cylinder in Hydraulic Piston Pump-Motor,'' ASME J. Tribol., **117**, pp. 80–85.
[12] Liu, K., Xie, Y. B., and Gui, C. L., 1998, ''A Comprehensive Study of the Friction and Dynamic Motion of the Piston Assembly,'' Proc. Inst. Mech. Eng., **212**, Part J, pp. 221–226.
[13] Fagotti, F., Todescat, M. L., Ferreira, R. T. S., and Prata, A. T., 1994, ''Heat Transfer Modeling in a Reciprocating Compressor,'' *Proceedings of the International Compressor Engineering Conference at Purdue*, West Lafayette, IN, pp. 605–610.
[14] Todescat, M. L., Fagotti, F., Prata, A. T., and Ferreira, R. T. S., 1992, ''Thermal Energy Analysis in Reciprocating Hermetic Compressors,'' *Proceedings of the International Compressor Engineering Conference at Purdue*, Vol. IV, West Lafayette, IN, pp. 1419–1428.
[15] Catto, A. G., and Prata, A. T., 1997, ''A Numerical Study of Instantaneous Heat Transfer During Compression and Expansion in Piston-Cylinder Geometry,'' *Proceedings of the ASME Advanced Energy System Division*, AES-Vol. 37, pp. 441–450.
[16] Prata, A. T., and Ferreira, R. T. S., 1990, ''The Accuracy of Short Bearing Theory in Presence of Cavitation,'' ASME J. Tribol., **112**, pp. 650–654.
[17] Dowson, D., and Taylor, C. M., 1979, ''Cavitation in Bearings,'' Annu. Rev. Fluid Mech., **11**, pp. 35–66.
[18] Gasche, J. L., Ferreira, R. T. S., and Prata, A. T., 1999, ''Transient Flow of the Oil-Refrigerant Mixture Through the Radial Clearance in Rolling Piston Compressor,'' *Proceedings of the ASME Advanced Energy System Division*, AES-Vol. 39, pp. 119–127.
[19] Gasche, J. L., Ferreira, R. T. S., and Prata, A. T., 2000, ''Two-Phase Flow of the Oil-Refrigerant Mixture Through the Radial Clearance in Rolling Piston Compressor,'' accepted to the *International Compressor Engineering Conference at Purdue*, West Lafayette, IN.